© 2016. Published by The Company of Biologists Ltd | Journal of Cell Science (2016) 129, 2106-2119 doi:10.1242/jcs.187120

RESEARCH ARTICLE

Together, the IFT81 and IFT74 N-termini form the main module for intraflagellar transport of tubulin

Tomohiro Kubo[1], Jason M. Brown[1,2], Karl Bellve[3], Branch Craige[1], Julie M. Craft[4], Kevin Fogarty[3], Karl F. Lechtreck[4] and George B. Witman[1,*]

ABSTRACT

The assembly and maintenance of most cilia and flagella rely on intraflagellar transport (IFT). Recent *in vitro* studies have suggested that, together, the calponin-homology domain within the IFT81 N-terminus and the highly basic N-terminus of IFT74 form a module for IFT of tubulin. By using *Chlamydomonas* mutants for IFT81 and IFT74, we tested this hypothesis *in vivo*. Modification of the predicted tubulin-binding residues in IFT81 did not significantly affect basic anterograde IFT and length of steady-state flagella but slowed down flagellar regeneration, a phenotype similar to that seen in a strain that lacks the IFT74 N-terminus. In both mutants, the frequency of tubulin transport by IFT was greatly reduced. A double mutant that combined the modifications to IFT81 and IFT74 was able to form only very short flagella. These results indicate that, together, the IFT81 and IFT74 N-termini are crucial for flagellar assembly, and are likely to function as the main module for IFT of tubulin.

KEY WORDS: Cilia, Flagella, *Chlamydomonas*, Microtubule, Ciliary assembly, Tubulin binding

INTRODUCTION

Intraflagellar transport (IFT) is a process in which large protein assemblies termed 'IFT trains' are moved anterogradely along the doublet microtubules of cilia and flagella (hereafter used interchangeably) by the microtubule motor kinesin 2, and retrogradely by the microtubule motor dynein 1b/2 (Rosenbaum and Witman, 2002; Scholey, 2008). The IFT trains are composed of complexes including IFT-A, which contains at least six different subunits, and IFT-B, which contains at least 16 different subunits (Bhogaraju et al., 2013a). Another large complex, the BBSome, contains eight Bardet–Biedl syndrome (BBS) proteins and, in many organisms, appears to be an IFT adaptor for the export of membrane proteins from the cilium (Eguether et al., 2014; Lechtreck et al., 2009; Lechtreck et al., 2013; Liew et al., 2014). The IFT complexes transport proteins that are necessary for the assembly and maintenance of cilia (Ishikawa and Marshall, 2011), and also move signals between the cilium and cell body (Eguether et al., 2014; Liem et al., 2012; Liew et al., 2014; Wang et al., 2006). Mutations in IFT motors and complex proteins cause defects in ciliary assembly and function, resulting in several human diseases, including Jeune asphyxiating thoracic dystrophy, short-rib polydactyly syndrome, Mainzer-Saldino syndrome and Ellis-van Creveld syndrome (Aldahmesh et al., 2014; Beales et al., 2007; Caparrós-Martín et al., 2015; Dagoneau et al., 2009; Davis et al., 2011; Halbritter et al., 2013; Huber et al., 2013; McInerney-Leo et al., 2013; Merrill et al., 2009; Perrault et al., 2012, 2015; Schmidts et al., 2013, 2015).

Although many axoneme, ciliary membrane and ciliary signaling proteins have been shown to be moved by IFT (Lechtreck, 2015), very little is known about which specific IFT complex proteins bind these cargos. Within IFT-B, which is the best-studied of the complexes, IFT46 has been implicated in transport of outer-arm dynein (Hou et al., 2007; Ahmed et al., 2008) and, together, IFT25 and IFT27 are involved in transport of the BBSome (Eguether et al., 2014). However, by far the most abundant protein in the cilium is tubulin, which is transported by IFT (Craft et al., 2015; Hao et al., 2011; Marshall and Rosenbaum, 2001) and is likely to be its main cargo. Recently, Bhogaraju et al. (2013b) provided evidence, primarily on the basis of structural analysis and *in vitro* experiments, that the IFT-B proteins IFT81 and IFT74 together form a tubulin-binding module for this transport. These two proteins are known to interact with each other through coiled-coil domains to form part of what is known as the IFT-B 'core' (Lucker et al., 2005; Taschner et al., 2011). Bhogaraju et al. (2013b) proposed that the N-termini of the two proteins project from the core. By solving the crystal structure of the IFT81 N-terminus and investigating the tubulin-binding affinity of the IFT81N–IFT74N heterodimer, Bhogaraju and colleagues showed that a calponin-homology domain within the N-terminus of IFT81 binds the globular body of tubulin with moderate affinity, and that the highly basic N-terminus of IFT74 interacts with the highly acidic tail (also known as E-hook) of β-tubulin to strengthen the binding affinity by ∼18 fold. The requirement for both IFT81 and IFT74 to achieve high-affinity binding to tubulin was predicted to result in low tubulin association with either protein prior to their assembly into an IFT-B complex. The high affinity of IFT81–IFT74 for tubulin (K_d=0.9 μM) was predicted to be within a range that would result in high tubulin occupancy of IFT complexes during early stages of flagellar regeneration but lower occupancy in steady-state flagella, thus providing a mechanism that is potentially important for the control of flagellar length. However, this proposal has yet to be rigorously tested *in vivo*.

The identification of *Chlamydomonas* mutants that are null for both IFT81 (this study) and IFT74 (Brown et al., 2015) have enabled us to directly test *in vivo* the importance of the N-termini of these two proteins in tubulin transport, by transforming the mutants with constructs that express versions of IFT81 and IFT74 in which the putative tubulin-binding regions are modified or removed. We found that either substitution of the five basic residues in the IFT81 N-terminus that Bhogaraju et al. (2013b) had predicted to be involved in tubulin binding or truncation of the IFT74 N-terminus that precedes the coiled-coil domain has little or no effect on basic

[1]Department of Cell and Developmental Biology, University of Massachusetts Medical School, Worcester, MA 01655, USA. [2]Biology Department, Salem State University, Salem, MA 01970, USA. [3]Biomedical Imaging Group, University of Massachusetts Medical School, Worcester, MA 01605, USA. [4]Department of Cellular Biology, University of Georgia, Athens, GA 30602, USA.

*Author for correspondence (George.Witman@umassmed.edu)

G.B.W., 0000-0002-9497-9218

Received 28 January 2016; Accepted 3 April 2016

Journal of Cell Science

Journal of Cell Science (2016) 129, 2106-2119 doi:10.1242/jcs.187120

anterograde IFT or the length of steady-state flagella. Nevertheless, either of these modifications slowed the rate of flagellar regeneration. Total internal reflection fluorescence (TIRF) microscopy of fluorescently tagged tubulin within regenerating flagella revealed that the mutations to either the N-terminus of IFT81 or the N-terminus of IFT74 greatly reduced anterograde transport of tubulin, indicating that, consistent with Bhogaraju et al. (2013b), the N-termini of both IFT81 and IFT74 are important for IFT of tubulin (hereafter referred to as tubulin IFT). However, some tubulin transport remained when IFT81 or IFT74 alone were modified. This residual tubulin transport and the ability of the cells to form normal or near-normal length flagella is likely to be mediated by the unmodified IFT74 or IFT81, because a strain carrying mutations within both the IFT81 and IFT74 N-termini formed only very short flagella. These results indicate that the N-termini of IFT81 and IFT74 form the main, and possibly sole, module for IFT of tubulin.

RESULTS

Identification of a *Chlamydomonas* IFT81-null mutant

In the ongoing process of isolating *Chlamydomonas* insertion mutants with defects in genes crucial for flagellar assembly and/or motility, we isolated strain 7F#5 that exhibits a palmelloid – i.e. failure to hatch from the mother cell wall – phenotype, which often is due to a defect in flagella formation (Fig. 1A). Indeed, when the cells were artificially hatched by treating them with the cell-wall-

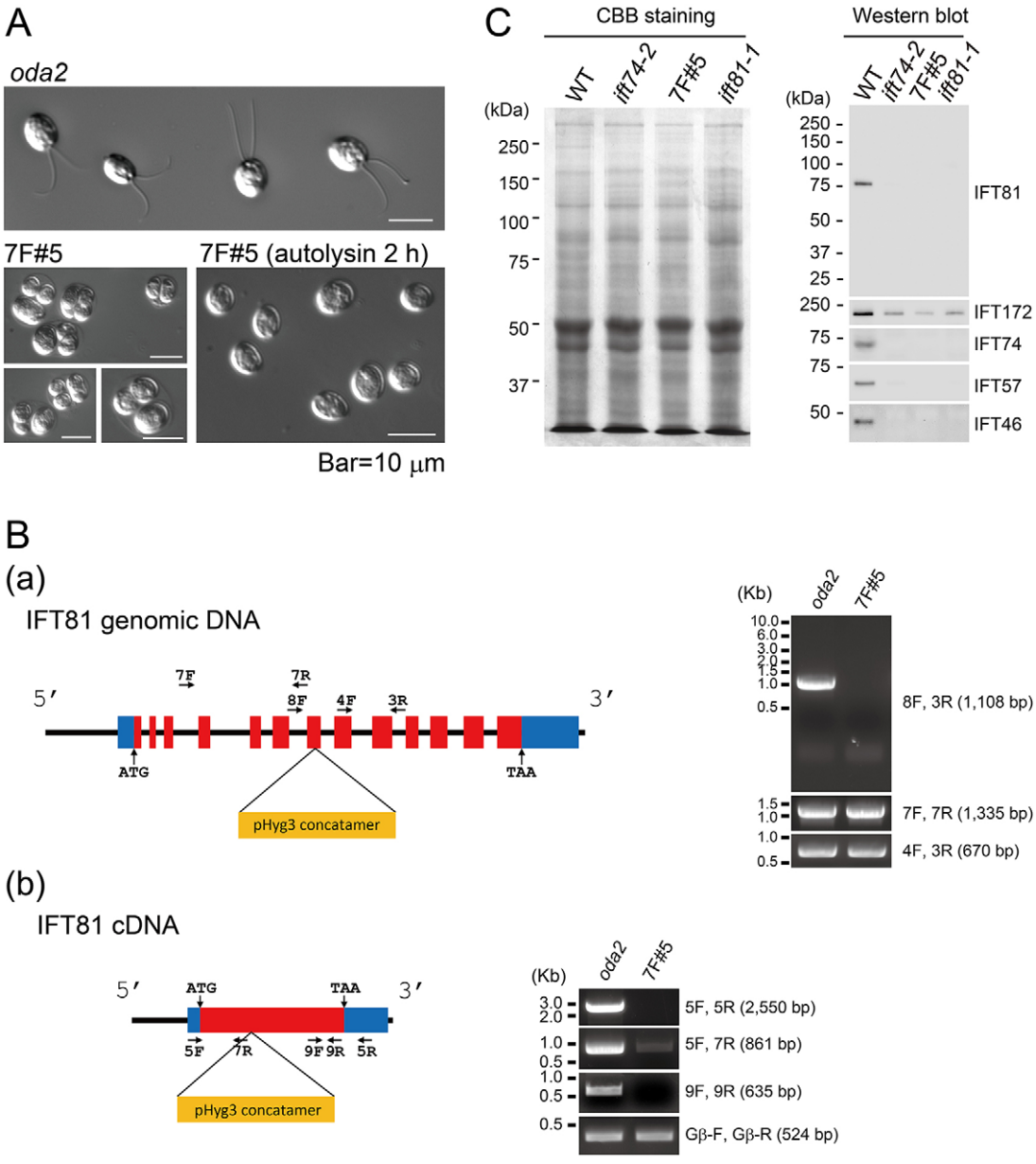

Fig. 1. A novel *Chlamydomonas* insertional mutant null for IFT81. (A) Differential interference contrast (DIC) microscopy of the 7F#5 transformant and its parent strain *oda2* treated with and without autolysin. The 7F#5 strain is palmelloid and does not form flagella, even after release from the mother cell wall by autolysin. (B) Schematic and PCR analyses of (a) genomic and (b) cDNA of *IFT81*. PCR analysis revealed that one or more copies of the hygromycin-resistance gene had inserted into exon 7 of *IFT81*. Amplification of cDNA by PCR confirmed that all or most IFT81 transcripts are absent in the 7F#5 mutant. (C) Coomassie Brilliant Blue (CBB)-stained SDS-PAGE gel (left) and western blot (right) of wild-type (WT), *ift74-2*, 7F#5 and *ift81-1* whole-cell extracts. The gel stained with CBB confirmed that an equal amount of protein was loaded in each lane.

Journal of Cell Science (2016) 129, 2106-2119 doi:10.1242/jcs.187120

digesting enzyme autolysin, none of the cells were flagellated. Moreover, in contrast to some other palmelloid strains (Craige et al., 2010; Kubo et al., 2015), none of the hatched cells subsequently grew flagella (Fig. 1A). These results suggest that this strain has a complete inability to assemble flagella.

Strain 7F#5 had been made by transformation of the strain *oda2*, which lacks outer dynein arms, with a fragment of the hygromycin-resistance gene pHyg3 (Berthold et al., 2002; see Materials and Methods). DNA sequencing of restriction enzyme site-directed amplification (RESDA)-PCR products (González-Ballester et al., 2005) revealed that the pHyg3 sequence had inserted into exon 7 of *IFT81* (Fig. 1Ba). This was confirmed by using specific primers and PCR to amplify IFT81 genomic sequences from purified *oda2* and 7F#5 DNA: the region including exons 7–9 was amplified from the *oda2* DNA but not from the 7F#5 DNA, whereas normal amounts of product were obtained from 7F#5 DNA by using primer pairs both upstream and downstream of the insertion site (Fig. 1Ba). To determine whether stable transcripts were produced from the mutated gene, we carried out PCR amplification by using the reverse transcription product as a template. All primer pairs yielded abundant product from *oda2* cDNA. By contrast, with 7F#5 cDNA, primers specific for the 5′ end of the *IFT81* cDNA yielded only a barely detectable amount of product, and primers specific for the 3′ end of the cDNA yielded no product (Fig. 1Bb). Finally, a monoclonal antibody specific for IFT81 (Cole et al., 1998) failed to detect any protein in western blots of 7F#5 cells (Fig. 1C). Taken together, these results indicate that 7F#5 is likely to be functionally null for IFT81.

Because strain 7F#5 carries the *oda2* mutation (Kamiya, 1988) and could carry undetected mutations in genes other than *ODA2* and *IFT81*, we backcrossed it twice with wild-type strains. We selected a progeny, hereafter named *ift81-1*, with the same palmelloid and aflagellate phenotype and the same IFT81 mutation as 7F#5. As was the case for 7F#5, IFT81 was not detected in western blots of *ift81-1* cell extracts (Fig. 1C).

IFT81 is necessary for IFT-B assembly

Western blot analysis of whole-cell extracts revealed that *ift81-1* also has greatly reduced levels of the IFT-B proteins IFT57 and IFT46 (Fig. 1C), which presumably are degraded within the cell body. This is indicative of a severe defect in IFT-B assembly (see Fig. 7) and, undoubtedly, accounts for the inability to form flagella. Interestingly, this phenotype is similar to that of *ift74-2*, which appears to completely lack IFT74 and also has a severe defect in the assembly of IFT-B (Brown et al., 2015 and Fig. 1C). Moreover, *ift81-1* cells have a greatly reduced amount of IFT74 (Fig. 1C and Fig. 7), and *ift74-2* cells have little or no IFT81 (Brown et al., 2015 and Fig. 1C). However, both mutants retain the IFT-B 'peripheral' protein IFT172 (Brown et al., 2015) and the IFT-A protein IFT139 (Brown et al., 2015) (Fig. 1C and Fig. 7, respectively) as well as IFT motors (T.K., unpublished results).

To confirm that the flagellar assembly and IFT-B defects of *ift81-1* were due specifically to loss of IFT81, we transformed it with a DNA fragment encoding IFT81 with a 3×hemagglutinin (HA) tag at its C-terminal end and containing a paromomycin-resistance gene as a selectable marker. Numerous transformants that had resistance to paromomycin were motile; one of these, named *ift81-1 IFT81HA*, was selected for further analysis and found to be fully rescued for flagella motility and length (Fig. 2A and B). As expected, western blot analysis of isolated flagella and whole-cell extracts of *ift81-1 IFT81HA* demonstrated that the slightly larger IFT81-HA was now present in place of IFT81, and that IFT-B as represented by IFT57 was now restored, although the flagella contained slightly less IFT-B than wild-type flagella (Fig. 2C). The normal motility and presence of the outer dynein arm intermediate chain IC2 in the flagella confirmed that the backcrosses had eliminated the *oda2* mutation present in 7F#5. To confirm that IFT81-HA was localized normally, wild-type and *ift81-1 IFT81HA* cells were doubly labeled with anti-acetylated α-tubulin and anti-HA antibodies. In contrast to wild-type cells, which had no obvious HA labeling, *ift81-1 IFT81HA* cells exhibited strong signal in the basal-body region and punctate signals along the flagella (Fig. S1A), as previously reported for wild-type IFT81 (Cole et al., 1998; Richey and Qin, 2012). Finally, anti-HA immunoprecipitation experiments using flagellar extracts from *ift81-1 IFT81HA* cells and *ift46-1 IFT46HA* cells (expressing IFT46 tagged with HA; Brown et al., 2015) showed that IFT81-HA was incorporated into IFT-B within the former cells at a stoichiometry similar to that of untagged IFT81 in the latter cells (Fig. S1B). Collectively, the above results confirm that the inability of *ift81-1* cells to assemble flagella is due to the mutation in *IFT81*, and that IFT81 is essential for assembly of IFT-B. The fact that *ift81-1* and *ift74-2* (Brown et al., 2015) have similar severe defects in the assembly of IFT-B is consistent with the model that these two proteins interact in order to form part of the IFT-B core.

IFT81 tubulin-binding domain mutants generate nearly full-length flagella

In the *Chlamydomonas* IFT81 calponin-homology domain, there are a total of five highly conserved basic residues (K73, R75, R85, K112 and R113, which correspond to human K73, K75, R87, K114 and R115, respectively) predicted to be involved in tubulin binding (Bhogaraju et al., 2013b). To examine the importance of these residues in flagellar assembly and tubulin transport, we transformed *ift81-1* with wild-type IFT81 or with six different constructs encoding versions of IFT81 in which one, two, three, four or all five of these basic residues were replaced by glutamate (Table S1). For simplicity, the latter strains will be referred to as *ift81-1 IFT81(1E)* to *ift81-1 IFT81(5E)*, and the products of the constructs will be referred to as IFT81(1E) to IFT81(5E), respectively. Western blot analysis of isolated flagella (Fig. 3A) and whole-cell extracts (Fig. S2A) of these strains showed that every one of the constructs restored IFT-B. Levels of IFT proteins in the whole cells were similar to those in wild type, whereas IFT protein levels in the flagella appeared to be lower than in wild type. Immunofluorescence microscopy showed that the rescued IFT-B complex was localized normally to the basal-body region and flagella even in the most severely substituted *ift81-1 IFT81(5E)* strain (Fig. 3B). Importantly, all of the constructs also rescued flagellar assembly in the *ift81-1* mutant, and the flagella were of normal or nearly normal length and motility (Fig. 3C,D and E; Fig. S2B,C). We also used differential interference contrast (DIC) microscopy to examine IFT in full-length (i.e. steady-state) flagella of the strains, and found that the velocities and frequencies of both anterograde and retrograde IFT particles were normal or nearly normal in all the strains (Fig. 3F). Therefore, the putative tubulin-binding residues in IFT81 are not essential for flagellar assembly, and mutation of these residues has no obvious effect on cycling of IFT particles in non-regenerating flagella.

IFT81 tubulin-binding domain mutants have slow flagellar regeneration kinetics

If there is a defect in tubulin transport in any of these strains, then one might expect to see an effect on the kinetics of flagellar formation. In *Chlamydomonas* this is easily assessed by deflagellating the cells and then measuring flagellar length as a

Journal of Cell Science (2016) 129, 2106-2119 doi:10.1242/jcs.187120

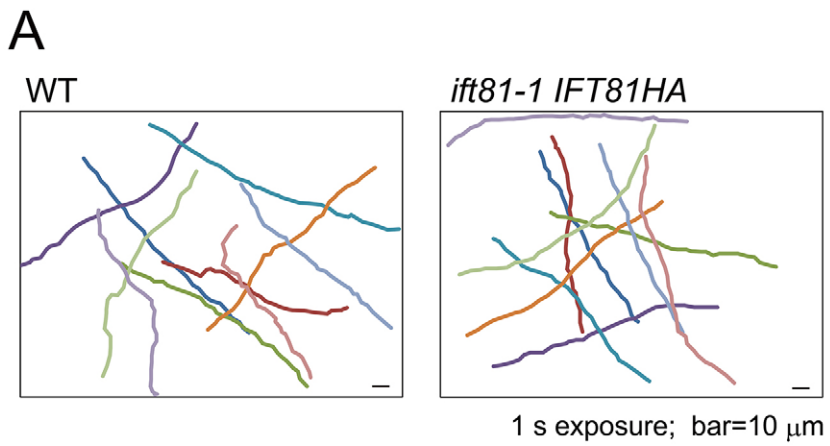

Fig. 2. Transformation of *ift81-1* with genomic IFT81 sequence rescues its phenotype. (A,B) Swimming trajectories and flagellar lengths of wild-type (WT) and *ift81-1 IFT81HA* cells. (C) Western blot of isolated flagella and whole-cell extracts of wild type (WT) and *ift81-1 IFT81HA*. IC2, an axonemal dynein intermediate chain missing in *oda2* flagella (T.K., unpublished result), is restored in *ift81-1 IFT81HA* flagella; α-tubulin served as a loading control.

function of time as the cells synchronously grow new flagella (Rosenbaum et al., 1969). When we did this, we found that strains *ift81-1 IFT81(1E)*, *ift81-1 IFT81(2E)* and *ift81-1 IFT81(2E′)* had normal flagellar regeneration kinetics (Fig. 4Aa,b). However, the rate of flagellar growth became progressively slower as three, four or five of the predicted tubulin-binding residues were substituted (Fig. 4Ab,c). The rates during the initial linear phase of flagellar regeneration were ∼51%, ∼67% or ∼36% of wild type in the strains with three, four or five substitutions, respectively. These results indicate that mutation of three or more of the five putative tubulin-binding residues of IFT81 cause slower flagellar regeneration and that, in general, the effect increases as the number of mutations increases, depending on the specific residues substituted.

Basic anterograde IFT is normal in regenerating flagella of *ift81-1 IFT81(5E)*

This slower flagellar growth might reflect a general problem with IFT during flagellar regeneration or might be due to a problem specifically with delivery of tubulin to the tip of the growing flagellum. To determine whether there is a general impairment of IFT during flagellar regeneration that may account for the slower regeneration kinetics, we again analyzed IFT particle movement by means of DIC microscopy, this time using half-grown flagella of *ift81-1 IFT81(5E)* and a control strain (Fig. 4B–D). As we had observed with steady-state flagella, anterograde and retrograde velocity were nearly normal, and anterograde and retrograde frequency were normal in the regenerating flagella of the *ift81-1 IFT81(5E)* strain. Therefore, the slower flagellar regeneration observed in the IFT81 calponin-homology domain mutants is not due to a general defect in IFT but might be due to a specific defect in tubulin transport within the flagella.

IFT74Δ130 lacks the predicted tubulin-binding domain of IFT74

A similar possibility was suggested to explain the slower flagellar regeneration kinetics of the strain *ift74-2 IFT74Δ130* that lacks the IFT74 N-terminus (Brown et al., 2015). The IFT74 N-terminus, which precedes the first coiled-coil domain, contains 22 positively charged residues that make this region highly basic (pI 12.18); this region is likely to be flexible and disordered in its 3D structure (Bhogaraju et al., 2013b). Consequently, removing this region should abolish the electrostatic interaction between IFT74 and the β-tubulin E-hook that is predicted to be important for tubulin binding.

ift74-2 IFT74Δ130 was generated by transforming the IFT74-null mutant *ift74-2* with a construct expressing a version of IFT74 that lacks the N-terminal 130 amino acids, including all those proposed to be involved in binding to tubulin but excluding those contributing to the coiled-coil domains necessary for interaction with IFT81. This protein is termed IFT74Δ130 and rescues the defect in IFT-B assembly observed in *ift74-2* (Brown et al., 2015, and see Figs 1C and 6A). The rescued cells form nearly full-length flagella (Brown et al., 2015, and see Fig. 6B), albeit at an initial rate of regeneration that is only about 22% of the rate of wild-type cells

Journal of Cell Science (2016) 129, 2106-2119 doi:10.1242/jcs.187120

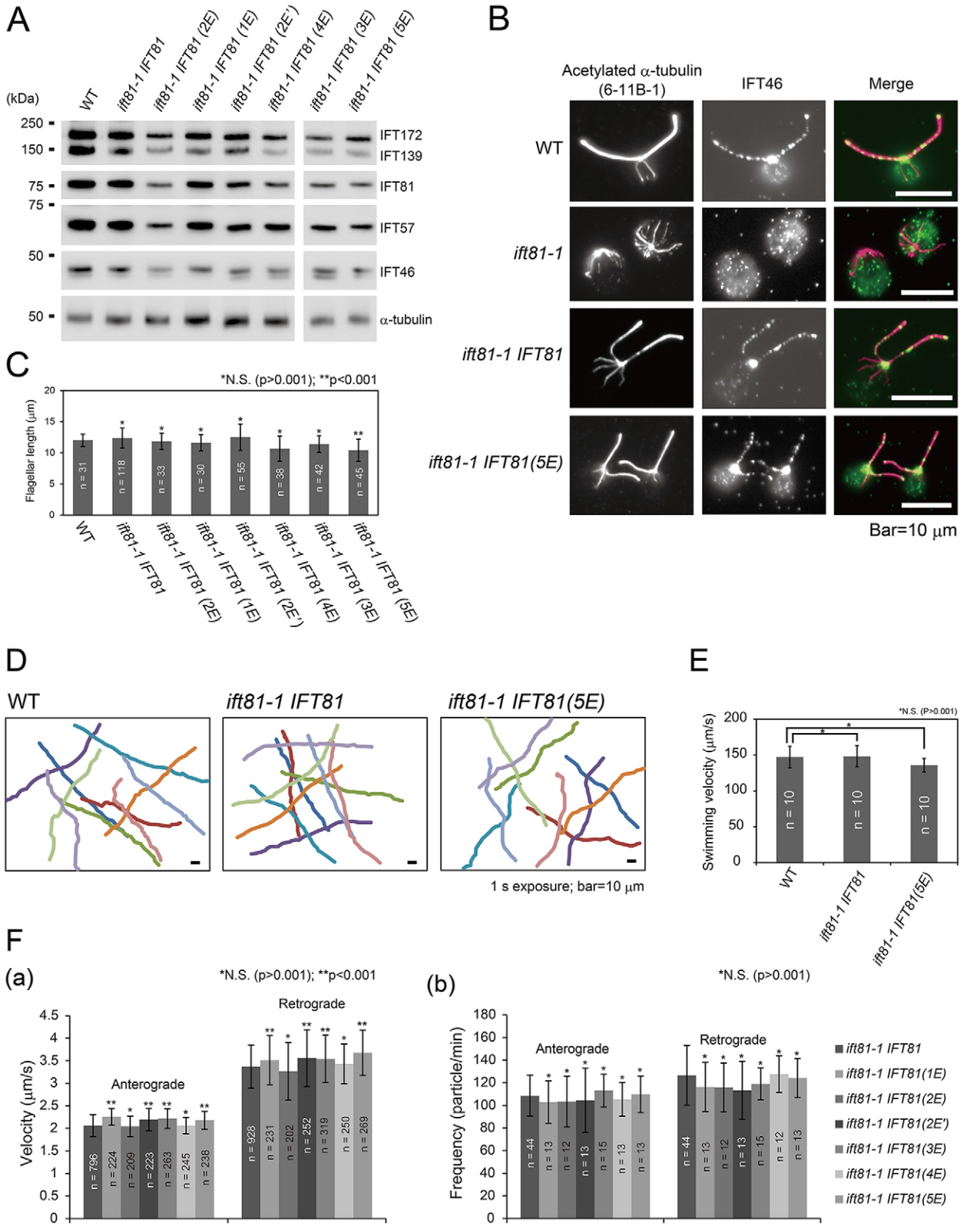

Fig. 3. Rescue of *ift81-1* with versions of IFT81 in which the predicted tubulin-binding residues are mutated. (A) Western blot of isolated flagella of wild type (WT) and the *ift81-1* mutant transformed with constructs expressing wild-type IFT81 or IFT81 in which one to five of the predicted tubulin-binding residues were replaced by glutamate. A similar blot showing the recovery of IFT-B in whole cells is shown in Fig. S2A. (B) Indirect immunofluorescence microscopy of WT, *ift81-1, ift81-1 IFT81* and *ift81-1 IFT81(5E)* cells doubly labeled with anti-acetylated α-tubulin and anti-IFT46 antibodies. Localization of the IFT-B protein IFT46 is normal in the *ift81-1 IFT81(5E)* strain. (C) Flagella of normal or nearly normal length (*ift81-1 IFT81(5E)*) are restored in all of the strains with substitutions in the tubulin-binding residues. (D,E) Swimming trajectories and velocities of wild-type (WT), *ift81-1 IFT81* and *ift81-1 IFT81(5E)* cells; data for other mutant strains are provided in Fig. S2B,C. (F) IFT-particle velocities (a) and frequencies (b) in steady-state flagella of the control and IFT81 tubulin-binding domain mutants as assessed by DIC microscopy.

Journal of Cell Science (2016) 129, 2106-2119 doi:10.1242/jcs.187120

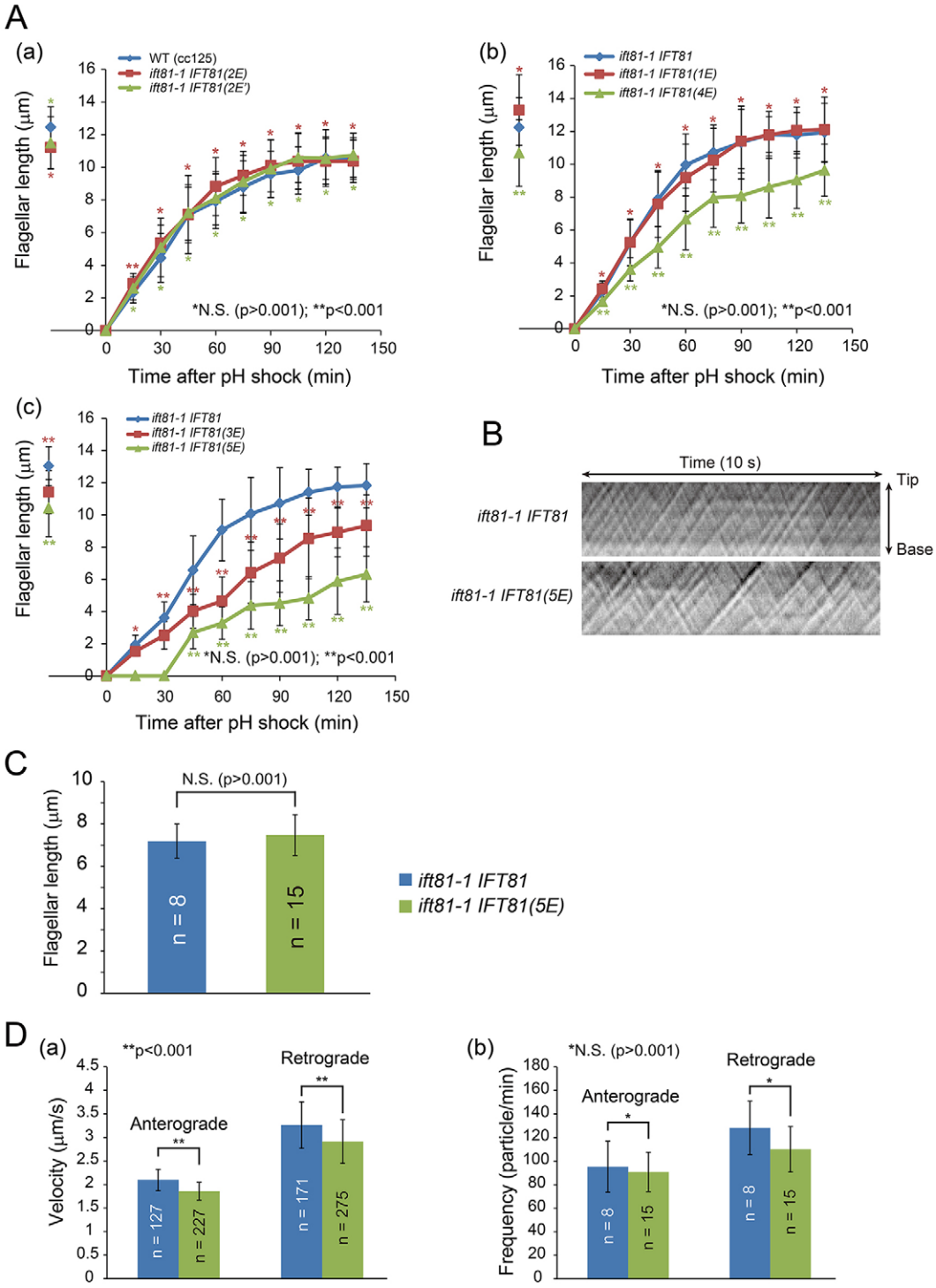

Fig. 4. Substitution of three or more of the predicted IFT81 tubulin-binding residues slows flagellar regeneration. (A) Kinetics of flagellar regeneration of IFT81 tubulin-binding domain mutants. Flagellar lengths prior to deflagellation are shown to the left of the y-axes; error bars show ±s.d. (B) Representative kymographs of IFT-particle movement in *ift81-1 IFT81* and *ift81-1 IFT81(5E)* during flagellar regeneration. (C) The regenerating flagella used for the kymographic analyses were about half-length during recording; the bars indicate the length (±s.d.) of those flagella that had been used to determine IFT-particle velocities and frequencies. (D) IFT-particle velocities and frequencies in *ift81-1 IFT81* and *ift81-1 IFT81(5E)* during flagellar regeneration.

(Brown et al., 2015). In steady-state flagella, anterograde IFT-particle velocity was about normal and anterograde IFT-particle frequency was ~75% compared with that of wild type, suggesting that there is no general defect in IFT that would explain the greatly reduced flagellar regeneration kinetics. However, no experiments were carried out to examine tubulin transport in this strain.

Frequency of tubulin transport is greatly reduced in mutants with defects in the proposed IFT81 or IFT74 tubulin-binding domain

Recently, Craft et al. (2015) established a technique to directly observe the translocation of fluorescently tagged α-tubulin within *Chlamydomonas* flagella by TIRF microscopy. We adopted this

Journal of Cell Science (2016) 129, 2106-2119 doi:10.1242/jcs.187120

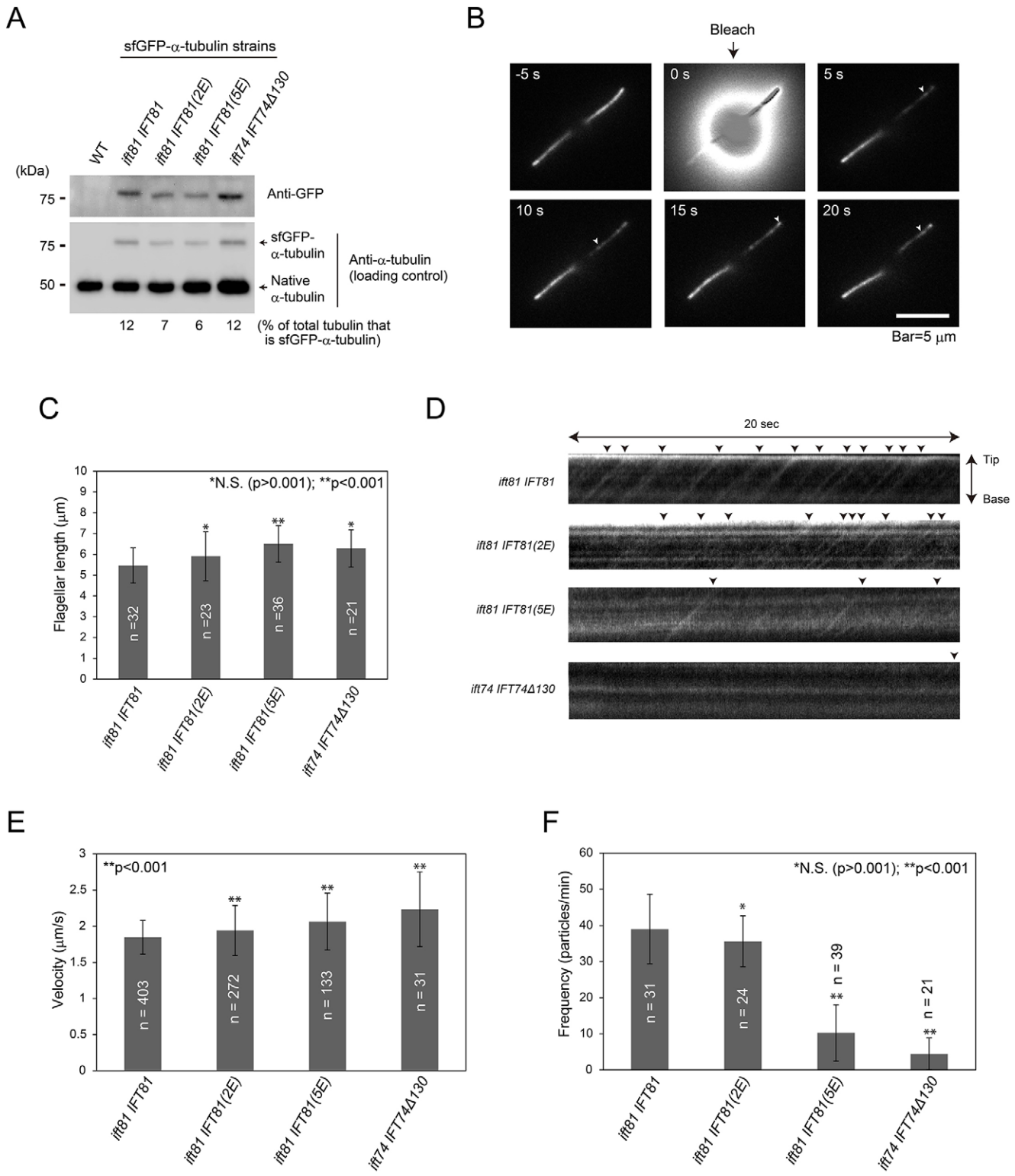

Fig. 5. Direct observation of tubulin transport in flagella. (A) Western blot analysis of whole-cell extracts of wild type (WT) and selected transformants expressing sfGFP–α-tubulin. For each strain, the percent of total tubulin represented by sfGFP–α-tubulin was estimated from the signal intensities of native and sfGFP–α-tubulin. (B) TIRF microscopy images of regenerating flagella illustrating bleach and IFT particles (arrowheads) that have entered the bleached flagellum. (C) Average length of regenerating flagella used for data collection. (D) Kymographs of tubulin transport in *ift81-1 IFT81* (control), *ift81-1 IFT81(2E)*, *ift81-1 IFT81 (5E)* and *ift74-2 IFT74Δ130* flagella. Arrowheads mark tracks of some fluorescent IFT particles. (E,F) Velocity and frequency of IFT-based tubulin transport for the indicated strains.

technique to assess the importance for tubulin transport of both the proposed IFT81 tubulin-binding residues and the IFT74 N-terminus. We expressed α-tubulin tagged with superfolder GFP (sfGFP–α-tubulin) in *ift81-1 IFT81*, *ift81-1 IFT81(2E)*, *ift81-1 IFT81(5E)* and *ift74-2 IFT74Δ130* cells. As expected (Craft et al., 2015), western blot analysis of whole-cell extracts showed different

Journal of Cell Science (2016) 129, 2106-2119 doi:10.1242/jcs.187120

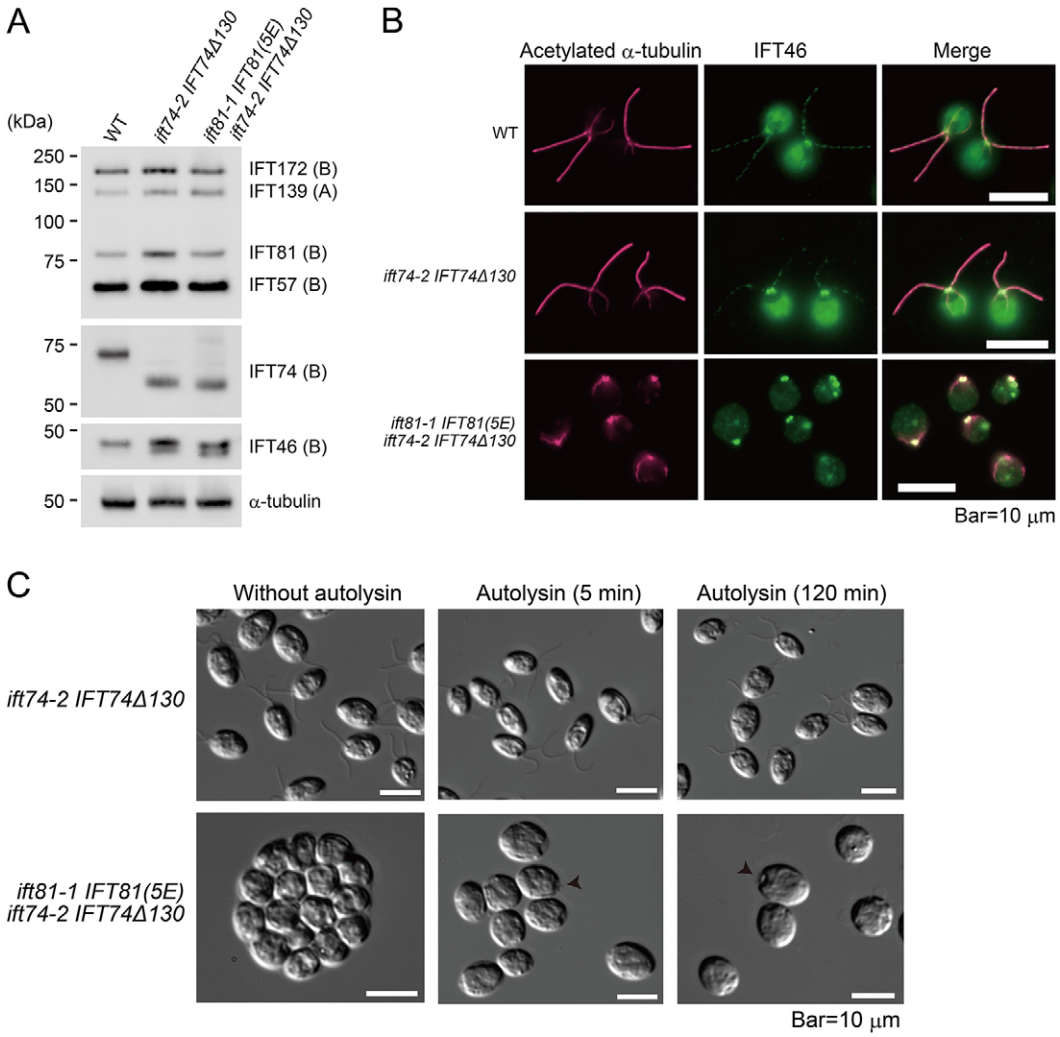

Fig. 6. The double mutant *ift81-1 IFT81(5E) ift74-2 IFT74Δ130* has a severe defect in flagella assembly. (A) Western blot of whole-cell extracts probed with the indicated antibodies. (B) Indirect immunofluorescence microscopy of the indicated strains doubly labeled with antibodies against acetylated α-tubulin and IFT46. The double mutant shows normal localization of IFT46 (representing IFT-B) in the basal-body region. *ift81-1 IFT81(5E) ift74-2 IFT74Δ130* cells were treated with autolysin to release cells from the palmelloid clusters; the other strains were treated identically. (C) DIC images of *ift74-2 IFT74Δ130*, which grows as single cells and has nearly full-length flagella, and of *ift81-1 IFT81(5E) ift74-2 IFT74Δ130*, which has a strong palmelloid phenotype. Following release of *ift81-1 IFT81(5E) ift74-2 IFT74Δ130* cells by autolysin treatment, very short flagella (arrowheads) are visible on some cells.

expression levels of sfGFP–α-tubulin among the different transformants (Fig. S3). To ensure that tubulin transport in the flagella of the strains to be analyzed would be comparable, we selected strains that had similar expression levels of sfGFP–α-tubulin ranging from 6–12% of total α-tubulin (Fig. S3; Fig. 5A).

Because tubulin transport occurs mainly during flagellar assembly (Craft et al., 2015), *ift81-1 IFT81*, *ift81-1 IFT81(2E)*, *ift81-1 IFT81(5E)* and *ift74-2 IFT74Δ130* cells expressing sfGFP–α-tubulin were deflagellated, and their regenerating flagella were observed by TIRF microscopy when they had grown to about half their normal length (Fig. 5B and C). Flagella that had stably attached to the coverslip were photobleached to reduce the strong fluorescence of the axoneme and, subsequently, recorded for 20 s to track transport of tubulin newly entering the flagella from the cell body (Fig. 5B); kymographs (Fig. 5D) were then made from the movies to facilitate quantitation of the movement. The velocity of anterograde tubulin transport was similar in all strains analyzed (Fig. 5E). Compared to the control, the frequency of anterograde tubulin transport was not significantly reduced in flagella of the *ift81-1 IFT81(2E)* mutant (Fig. 5F; compare Movies 1 and 2). However, the frequencies of tubulin transport in the flagella of the *ift81-1 IFT81(5E)* and *ift74-2 IFT74Δ130* mutants were reduced to only 26% and 11%, respectively, compared to that of the control (Fig. 5F; Movies 3 and 4). These results clearly demonstrate that the mutations in the proposed IFT81 tubulin-binding residues and the IFT74 N-terminus affect tubulin transport within flagella. This reduction in tubulin transport is likely to account for the comparable reduction in flagellar regeneration kinetics in these strains.

Combining the *IFT81(5E)* and *IFT74Δ130* mutations eliminates almost all flagellar assembly

Although the modifications to IFT81 and IFT74 both reduced tubulin transport, neither modification completely eliminated it. This raised the question of whether the residual tubulin transport in the *ift81-1 IFT81(5E)* flagella is mediated by the unmodified IFT74 and the residual tubulin transport in the *ift74-2 IFT74Δ130* flagella is mediated by the unmodified IFT81, or whether the residual transport is due to tubulin binding to some other IFT

Journal of Cell Science (2016) 129, 2106-2119 doi:10.1242/jcs.187120

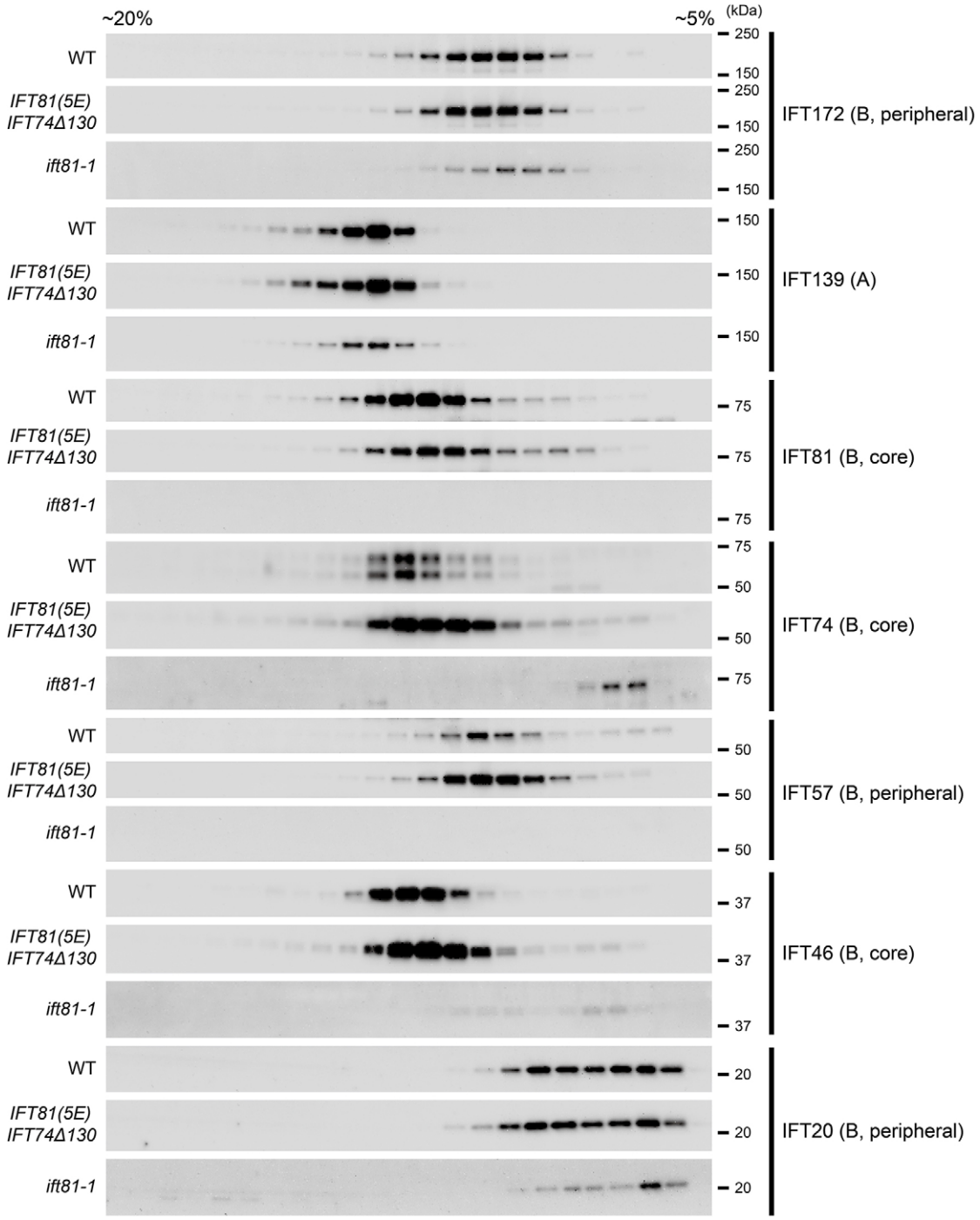

Fig. 7. IFT sub-complexes are assembled normally in the *ift81-1 IFT81(5E) ift74-2 IFT74Δ130* double mutant. Whole-cell lysates of wild type (WT), *ift81-1 IFT81(5E) ift74-2 IFT74Δ130* and *ift81-1* were fractionated by sucrose density gradient centrifugation. Cells of *ift81-1* lack IFT81 and have greatly reduced amounts of IFT74, IFT57 and IFT46; moreover, the residual IFT74 and IFT46 show an abnormal sedimentation profile. In contrast, all IFT proteins examined from *ift81-1 IFT81(5E) ift74-2 IFT74Δ130* cells had sedimentation profiles similar to those of the same proteins from wild-type cells. In the gradients of wild-type and double-mutant lysates, IFT172 and IFT57 peaked together but in different fractions from the IFT-B core components, suggesting that IFT172 and IFT57 are tightly associated with each other. The double band observed for wild-type IFT74 is probably due to protein degradation during preparation of the whole-cell lysate because it was not observed in wild-type whole-cell extracts prepared without NP-40 treatment and sonication (Fig. 6A and see Materials and Methods).

protein. To address this, we combined IFT81(5E) with IFT74Δ130 in a background otherwise null for both IFT81 and IFT74 (see Fig. S4; Materials and Methods). Western blotting of whole-cell extracts indicated that the resulting strain, termed *ift81-1 IFT81(5E) ift74-2 IFT74Δ130* 'double mutant', expressed IFT172, IFT139, IFT81, truncated IFT74, IFT57 and IFT46 (Fig. 6A). Moreover, in sucrose-density gradient centrifugation analysis of whole-cell lysates (Fig. 7), we observed no differences between wild type and the double mutant with regard to the sedimentation profiles of the IFT-particle proteins examined, including IFT81, IFT74 and IFT46, indicating that the proteins are likely to assemble into a normal IFT-B complex. Finally,

Journal of Cell Science (2016) 129, 2106-2119 doi:10.1242/jcs.187120

immunofluorescence microscopy of the double-mutant cells revealed that IFT46 localized normally to the basal-body region, as in wild-type or *ift74-2 IFT74Δ130* cells (Fig. 6B). Nevertheless, in contrast to the *ift81-1 IFT81(5E)* or *ift74-2 IFT74Δ130* 'single' mutants that hatch from the mother cell wall and have nearly full-length flagella, the double mutant has a strong palmelloid phenotype, suggesting a severe defect in flagellar assembly (Fig. 6C). Indeed, when the double-mutant cells were artificially hatched with autolysin, flagella were visible in only about 8% of cells and these flagella were very short – typically <1 µm (Fig. 6C). Therefore, concomitant loss of both the IFT81-tubulin-binding residues and the IFT74 N-terminus precludes any significant flagellar assembly. This suggests that the residual tubulin transport seen in the *ift81-1 IFT81(5E)* strain was due to the unmodified IFT74, and that the residual transport seen in the *ift74-2 IFT74Δ130* strain was due to the unmodified IFT81.

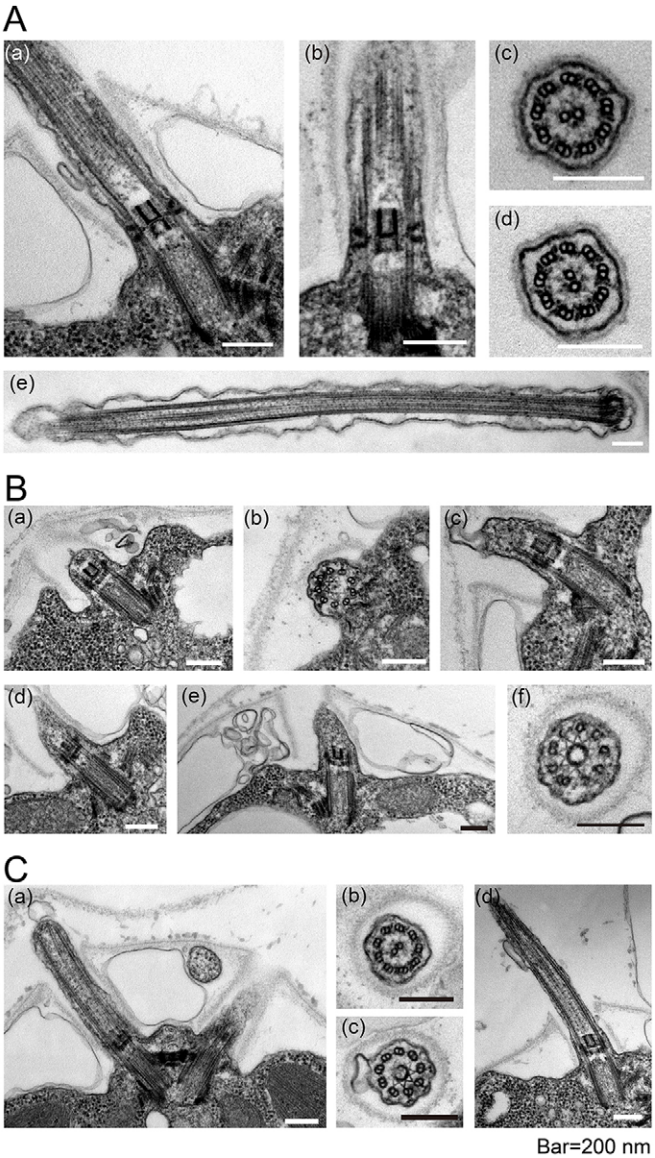

Fig. 8. Ultrastructure of wild-type, *ift81-1* and *ift81-1 IFT81(5E) ift74-2 IFT74Δ130* flagellar apparatuses. (A–C) Electron micrographs of (A) wild-type, (B) *ift81-1* and (C) *ift81-1 IFT81(5E) ift74-2 IFT74Δ130* cells. Cells of *ift81-1* completely fail to generate an axoneme. However, *ift81-1 IFT81(5E) ift74-2 IFT74Δ130* cells build a short axoneme with normal ultrastructure.

The ultrastructure of the very short *ift81-1 IFT81(5E) ift74-2 IFT74Δ130* flagella is normal

Electron microscopy revealed that, compared to wild-type cells (Fig. 8A), cells of *ift81-1* had normal basal bodies but the distal portion of the transition zone seemed to be incompletely formed, and doublet microtubules were never present distal to the transition zone (Fig. 8B). Instead, the space between the distal end of the transition zone and the flagellar membrane often contained small accumulations of particulate material (Fig. 8Bc–e). These results confirm that *ift81-1* is completely unable to assemble flagella. In contrast, in all sections of *ift81-1 IFT81(5E) ift74-2 IFT74Δ130* cells containing a longitudinally sectioned basal body, the basal body was connected to an apparently normal transition zone and axoneme (Fig. 8C). Therefore, most, if not all, cells of *ift81-1 IFT81(5E) ift74-2 IFT74Δ130* form flagella, but most of these flagella are too short to be observed by light microscopy. In both longitudinal and cross sections of these short flagella, the axonemes had an apparently normal ultrastructure, including outer doublet and central microtubules, outer dynein arms, inner dynein arms, and radial spokes. These results indicate that at least some tubulin is able to enter the *ift81-1 IFT81(5E) ift74-2 IFT74Δ130* flagella and assemble into short axonemal microtubules. Interestingly, this double mutant differs from many other IFT mutants in that there is no accumulation of IFT particles in the flagella.

DISCUSSION

In this study, we used a novel *Chlamydomonas* mutant that is null for IFT81, as well as a recently described mutant that is null for IFT74 (Brown et al., 2015), as starting points to dissect the role of the IFT81–IFT74 tubulin-binding module proposed to form the basis for transport of tubulin within the flagellum (Bhogaraju et al., 2013b). Mutation of the predicted tubulin-binding residues in the IFT81 N-terminus or elimination of the IFT74 N-terminus did not greatly affect IFT in general, but did greatly reduce IFT of tubulin. Concomitant with the reduction in tubulin transport, flagellar regeneration was slowed, although full-length flagella eventually formed. Combining the lesions to IFT81 and IFT74 within the same cell caused an even more severe flagellar assembly defect, such that only very short flagella (≤1 µm) were formed. These results support the hypothesis that the N-termini of these two proteins together form a tubulin-binding module (Bhogaraju et al., 2013b) and suggest that this is the main tubulin-binding module for IFT of tubulin. However, the formation of even very short flagella in cells with combined defects in IFT81 and IFT74 raise provocative questions about IFT, tubulin transport versus diffusion, and axonemal stability.

Loss of IFT81 or IFT74 affects IFT-B stability differently

Since IFT74 and IFT81 are known to directly interact with each other to form part of the IFT-B core (Lucker et al., 2005; Taschner et al., 2011), the lack of either protein might be expected to cause a similar defect in the assembly of IFT-B, resulting in identical phenotypes. However, although both strains grow in palmelloid clumps, *ift74-2* and *ift81-1* differ in their ability to form flagella. When the mother cell wall was removed by autolysin, ∼30% of *ift74-2* cells had very short flagella (often <1 µm long) (Brown et al., 2015). This phenotype is similar to that of *ift46-1*, which is null for IFT46 (Hou et al., 2007). In contrast, *ift81-1* fails to assemble any flagella, even after treatment with autolysin (Fig. 1A); this was confirmed by EM, which revealed that there is no extension of axonemal microtubules beyond the transition zone (Fig. 8B). The latter phenotype is similar to that of *bld1-1*, a mutant lacking IFT52 (Brazelton et al., 2001). The contrasting phenotypes of these two

Journal of Cell Science (2016) 129, 2106-2119 doi:10.1242/jcs.187120

pairs of mutants might reflect differences in the degree to which the remaining IFT-B proteins are degraded and/or the ability of the residual IFT-B proteins to assemble into a partially functional IFT-B complex – two aspects of IFT protein expression that are likely to be closely related. Although IFT-B core proteins are greatly reduced in amount within *ift74-2* and *ift46-1*, many of these proteins can still be detected by western blotting (see figure 2B in Brown et al., 2015 and figure 5 in Hou et al., 2007). In contrast, few IFT-B core proteins were detected within *ift81-1* (Fig. 1C) or *bld1-1* (Richey and Qin, 2012). Moreover, sucrose-density gradient centrifugation showed that *ift81-1* and *bld1-1* also have a severe defect in the assembly of IFT-B (Fig. 7 and Richey and Qin, 2012), whereas IFT46 has been reported not to be essential for assembly of the residual IFT-B proteins into a complex (Richey and Qin, 2012).

The IFT81–IFT74 tubulin-binding module is likely to be the main tubulin-binding site for IFT of tubulin

We found that both the *ift81-1 IFT81(5E)* and the *ift74-2 IFT74Δ130* mutant can still transport tubulin and build full-length or nearly full-length flagella. However, when both modifications were combined in the same cell, the cell was able to assemble only very short flagella. Although it was impossible to directly examine tubulin transport in these very short flagella, this result suggests that tubulin IFT in *ift81-1 IFT81(5E)* cells is mediated by IFT74, and that tubulin IFT in *ift74-2 IFT74Δ130* cells is meditated by IFT81. Alternatively, the tubulin-binding domains of IFT81 and IFT74 might interact in such a way that some cooperative function remains when either protein alone is mutated. In either case, if the residual tubulin IFT and ability to form normal-length flagella in *ift81-1 IFT81(5E)* and *ift74-2 IFT74Δ130* were due to tubulin binding outside of the IFT81–IFT74 tubulin-binding module, then it should have been possible for the *ift81-1 IFT81(5E) ift74-2 IFT74Δ130* double-mutant cells to form full-length flagella.

Within IFT-B, there are three proteins (IFT57, IFT54 and IFT38) in addition to IFT81 that have calponin-homology domains and could interact with tubulin or actin (Bhogaraju et al., 2014). Recent *in-vitro*-binding studies, in which bacterially expressed *Chlamydomonas* proteins were used, indicate that IFT38 and IFT57 do not bind tubulin but IFT54 binds soluble tubulin with a K_d within the low μM range, similar to that of IFT81–IFT74 (Taschner et al., 2016). This finding is in agreement with a previous report that the calponin-homology domain of mammalian IFT54 binds to both tubulin and taxol-stabilized microtubules *in vitro* (Ling and Goeddel, 2000). Therefore, it is possible that IFT54 also is involved in IFT of tubulin. However, if this is the case, its contribution to total tubulin IFT is likely to be very small compared to that of the IFT81–IFT74 tubulin-binding module. Our findings that tubulin IFT is reduced by 74% and 89% following mutation of the IFT81 and IFT74 N-termini, respectively, and that only very short flagella are formed when the modifications to these two proteins are combined in the same cell, strongly suggest that the IFT81–IFT74 tubulin-binding module is the main site of tubulin binding for IFT.

Neither component of the proposed tubulin-binding module is essential for tubulin IFT

Although the IFT81–IFT74 tubulin-binding module appears to be the main site for tubulin binding for IFT, our results indicate that the tubulin-binding domain of neither protein alone is essential for tubulin IFT. This result is not in disagreement with the model of Bhogaraju et al. (2013b). Bhogaraju and colleagues determined experimentally that the human IFT81 N-terminus and the IFT81N–IFT74N heterodimer bound tubulin with a K_d of 16 μM and 0.9 μM, respectively. Assuming an intracellular tubulin concentration within the low μM range that increases with induction of tubulin synthesis upon onset of ciliogenesis, and using the equation $O_{IFT}=[Tub]/\{K_d+[Tub]\}$, where O_{IFT} is the fraction of IFT bound to tubulin and [Tub] is the local concentration of free tubulin at the base of the cilium, they predicted that most IFT complexes are occupied by tubulin early in regeneration when the free tubulin concentration is highest, but that progressively fewer IFT complexes are occupied later when the tubulin pool is depleted, leading to slowing and eventually cessation of cilia growth. The assumption that intracellular tubulin concentration is within the low μM range was based on measurements in vertebrate cells (Hiller and Weber, 1978), and the tubulin concentration at the site of IFT cargo loading in *Chlamydomonas* might well be higher. Indeed, Craft et al. (2015) more recently estimated that the concentration of soluble tubulin in the *Chlamydomonas* cell body is ∼50 μM. Although such estimates are only approximate because the cellular volume accessible to free tubulin is unknown, this value predicts that the fraction of IFT81 bound to tubulin is ∼0.75 in the *Chlamydomonas ift74-2 IFT74Δ130* cell body, where IFT loading occurs. The fact that we observed an ∼89% reduction in tubulin transport within *ift74-2 IFT74Δ130* flagella suggests either that *Chlamydomonas* IFT81 has a lower affinity for tubulin than does human IFT81 or that the intracellular tubulin concentration in *Chlamydomonas* is not as high as estimated by Craft et al. (2015), but still high enough to allow some transport by IFT81 alone. The affinity for tubulin of the IFT74 N-terminus is not known but it might be higher than that of the IFT81 N-terminus, given that loss of the former has a more severe effect on tubulin transport than mutation of the latter.

Interestingly, mutation of the five predicted tubulin-binding residues in IFT81 or elimination of the IFT74 N-terminus reduced detectable IFT of tubulin by 74% or 89%, respectively. However, these same modifications reduced the rate of flagellar regeneration by only 64% or 78%, respectively. There are at least two possible explanations for the less-severe effect on flagellar regeneration as compared to tubulin transport, and they are not mutually exclusive. The most likely scenario is that free tubulin dimers, which were not followed in our kymographic analyses, diffuse into the flagellum (Craft et al., 2015), thereby contributing to flagellar growth and allowing faster regeneration than that which could be supported by the residual tubulin IFT alone. Another possibility is that the lower affinity of tubulin for the modified tubulin-binding module reduces the number of GFP-tubulins on some IFT trains to below the detection limit of our system, so that some GFP-tubulin IFT was not recorded. The fact that the flagellar regeneration rate and the frequency of tubulin transport were more reduced in *ift74-2 IFT74Δ130* than in *ift81-1 IFT81(5E)* suggests that, even though both domains are involved in tubulin transport, the IFT74 N-terminus is more important for this than the IFT81 calponin-homology domain – as might be the case if the IFT74 N-terminus has a higher affinity for tubulin than the IFT81 calponin-homology domain.

The tubulin-binding module appears to function only for tubulin binding and transport

Although tubulin transport was severely reduced by truncation of the IFT74 N-terminus or mutation of the five IFT81 calponin-homology domain residues that were predicted to be involved in tubulin binding, the mutated strains still assembled flagella that, at steady state, were nearly full length and had normal motility and nearly normal anterograde IFT (Fig. 3; Brown et al., 2015). Therefore, it is unlikely that these strains have defects in aspects of

Journal of Cell Science (2016) 129, 2106-2119 doi:10.1242/jcs.187120

flagellar assembly other than tubulin transport. This is noteworthy because calponin-homology domains have been reported to interact with actin (Castresana and Saraste, 1995) as well as tubulin (Ciferri et al., 2008; Bhogaraju et al., 2013b), and actin is a subunit of some inner-arm dyneins (Kato-Minoura et al., 1997). Thus, there was a possibility that the IFT81 calponin-homology domain was involved in the transport of inner-arm dyneins into the flagellum. However, our results indicate that at least the five basic calponin-homology domain residues that are mutated in IFT81(5E) are not involved in dynein transport.

Tubulin entry by diffusion is not sufficient for flagellar formation

The double mutant *ift81-1 IFT81(5E) ift74-2 IFT74Δ130* builds very short flagella that clearly contain microtubules (Fig. 8). Therefore, a small amount of tubulin is entering these flagella, possibly by (1) diffusion, (2) binding to tubulin-binding domain(s) of IFT-particle protein(s) other than IFT81–IFT74 (e.g. the IFT54 calponin-homology domain), or (3) residual binding to the modified IFT81–IFT74 tubulin-binding module. The axonemes of these cells appear to have a normal ultrastructure, with outer dynein arms, inner dynein arms, etc. As these very large axonemal substructures are known to be dependent upon IFT for their entry into the flagellum (Piperno et al., 1996; Hou et al., 2007; Lechtreck, 2015), IFT is likely to still function in these cells, consistent with the apparently normal assembly and localization of the IFT-B complex in the double-mutant cytoplasm (Figs 6 and 7). Interestingly, there does not appear to be a large surplus of axonemal precursors in these flagella, suggesting that cargos in excess of assembled axonemal microtubules are removed from the flagellum by means of IFT. The absence of any accumulation of IFT particles between the axoneme and the flagellar membrane also suggests that IFT cycling is normal in these flagella.

It is of interest to compare the ultrastructure of these double-mutant cells with those of the *ift81-1* null mutant, which completely fails to assemble flagellar microtubules beyond the transition zone. If tubulin can enter the flagellum by diffusion (Craft et al., 2015), why are these cells unable to form flagella? Since these cells lack a normal IFT-B complex, the most likely option is that axonemal substructures – such as outer and inner dynein arms, which are known to be necessary for outer doublet stability (Kubo et al., 2015) – are not imported into the nascent flagella. In the absence of these substructures, outer doublet microtubules might not be stable enough to elongate, even in the presence of tubulin at concentrations otherwise adequate to support some axonemal growth. If this is the case, the axonemal substructures – which enter flagella concomitantly with tubulin throughout flagellar assembly – would be essential for flagellar elongation, and the import of these components would be a main raison d'être for IFT.

MATERIALS AND METHODS

Strains and cultures

The *C. reinhardtii* strains used were wild-type (cc124 and cc125), *oda2* (CC-2230, mt+), *ift46-1 IFT46HA* (Brown et al., 2015) and *ift74-2 IFT74Δ130* (Brown et al., 2015). Cells were cultured in liquid minimal (M) medium I (Sager and Granick, 1954) and aerated with 5% CO_2 or grown on Tris-acetate-phosphate (Gorman and Levine, 1965) agar plates. Cells were maintained on a 14-10 h light-dark cycle.

Generation and identification of the *ift81-1* insertional mutant

To generate insertional mutants, the *oda2* strain carrying a mutation in the gene encoding the outer arm dynein gamma heavy chain (Kamiya, 1988) was transformed with the 1.7-kb *Hind* III fragment of pHyg3, which confers hygromycin resistance (Berthold et al., 2002; Brown et al., 2012, 2015). Strains with palmelloid phenotypes – including 7F#5 (*oda2*; *ift81-1*) – were selected and their insertion sites were determined by DNA sequencing of products amplified by RESDA-PCR (González-Ballester et al., 2005). 7F#5 was backcrossed twice with wild-type strains (cc124 and cc125) to remove the *oda2* mutation and other mutations potentially caused by additional pHyg3 insertions. Transformation of the resulting strain (*ift81-1*, mt+, palmelloid) with the *Kpn*I fragment of pLC8-IFT81-aphVIII (see next section) yielded transformants that can properly generate flagella with normal motility, confirming that the phenotype is due to the mutation of IFT81.

Generation of strains expressing modified proteins

A 6-kb fragment of genomic sequence including the *IFT81* gene (Cre17.g723600, from 806 bp upstream of the 5′ UTR to 66 bp downstream of the 3′ UTR) was amplified by PCR using specific primers (Table S2). The resulting PCR product was ligated into the pGEM-T Easy vector (Promega) and sequenced. The IFT81 fragment was then excised by *EcoR*I and inserted into the multi cloning site (MCS) of the pLC8-MCS-aphVIII vector (a kind gift from Dr Haru-aki Yanagisawa) to generate pLC8-IFT81-aphVIII.

To tag IFT81 with hemagglutinin (HA), an *Nru*I site (TCGCGA) was introduced just before the stop codon of the IFT81 coding sequence in pLC8-IFT81-aphVIII and the *Nru*I/*Sca*I fragment of p3×HA (Silflow et al., 2001) was inserted into that site. To make various IFT81 tubulin-binding domain mutants, bases encoding the predicted IFT81 tubulin-binding residues were replaced with bases encoding glutamate residues by inverse PCR using specific primers (Table S2), followed by restriction enzyme digestion and ligation of the mutated DNA fragments into the original pLC8-IFT81-aphVIII vector. The introduced mutations were confirmed by sequencing.

All the constructed plasmids [pLC8-IFT81-aphVIII, pLC8-IFT81HA-aphVIII, pLC8-IFT81(R85E)-aphVIII, pLC8-IFT81(K73R75/EE)-aphVIII, pLC8-IFT81(K112R113/EE)-aphVIII, pLC8-IFT81(R85K112R113/EEE)-aphVIII, pLC8-IFT81(K73R75K112R113/EEEE)-aphVIII and pLC8-IFT81(K73R75R85K112R113/EEEEE)-aphVIII] were digested with *Kpn*I, and the resulting ∼8.6-kb fragments containing IFT81 genomic sequence with the paromomycin-resistance cassette were used to transform *ift81-1* by electroporation (Brown et al., 2012). Individual paromomycin-resistant transformants were picked, screened for motility and then analyzed by western blotting to select one strain for each construct in which the modified IFT81 is expressed at near wild-type levels.

The double mutant *ift81-1 IFT81(5E) ift74-2 IFT74Δ130* was made by mating *ift81-1 IFT(5E)* and *ift74-2 IFT74Δ130* using standard methods (Harris, 2009). Among multiple progenies that resulted from the mating of these two strains, PCR and DNA sequencing analyses were used to identify three strains that carry both *IFT81(5E)* and *IFT74Δ130* in a background otherwise null for *IFT81* and *IFT74* (Fig. S4).

Preparation of protein samples

For gel electrophoresis and western blotting, whole-cell extracts were prepared according to Fowkes and Mitchell (1998). Cells were collected by centrifugation and extracted by using methanol and chloroform. Subsequently, the precipitated products were washed twice with methanol. Cytoplasmic proteins were solubilized in a buffer containing 5 M urea, 2 M thiourea and 0.05% Triton X-100 (New England Nuclear).

Flagella were isolated according to Witman et al. (1978). For immunoprecipitation, flagella were extracted with 0.05% NP-40 (NP-40 alternative, Calbiochem #492018) in HMDEK (30 mM HEPES, 5 mM $MgSO_4$. 1 mM DTT, 0.1 mM EGTA, 25 mM CH_3COOK). The extracts were centrifuged to remove axonemes and the supernatants were collected and diluted with a 10× volume of immunoprecipitation buffer (10 mM HEPES, 5 mM $MgCl_2$, 1 mM DTT, 0.1 mM EDTA, 25 mM KCl, 75 mM NaCl and 1.5% polyvinylpyrrolidone 40). Antibodies against the HA tag (Covance, rabbit polyclonal antibody HA.11; Roche, rat monoclonal antibody 3f10) conjugated with protein-G agarose (Life Technologies) were mixed with samples and agitated for 2 h at 4°C. The agarose beads were then washed three times with immunoprecipitation buffer followed by SDS-PAGE and western blotting.

For preparation of cell lysates for sucrose density gradient centrifugation, cells were concentrated by centrifugation (Sorval RC-3B, H-6000A rotor,

3000 rpm, 5 min) and resuspended in M medium with autolysin for 1 h (Craige et al., 2010). The cells were then collected by centrifugation as above and lysed by resuspension in HMDEK containing 1% NP40 followed by sonication at 4°C (Branson Sonifier 250; ten pulses at '30%' duty cycle and '5' output control). The lysate was clarified by centrifugation (Sorval SS-34 rotor, 15,000 rpm, 10 min, 4°C) and layered over 12-ml 5–20% sucrose density gradients in HMDEK. The gradients were centrifuged at 36,000 rpm (Beckman SW 41 rotor) for 12.5 h at 4°C and fractionated into 23 aliquots.

SDS-PAGE and western blotting

Flagellar and cytoplasmic proteins were separated by SDS-PAGE on 7.5% or 4–15% gradient gels (Bio-Rad). Gels were stained with Coomassie Brilliant Blue or silver. Western blots were performed according to Towbin et al. (1979). Primary antibodies used in this study are listed in Table S3.

Immunofluorescence and DIC microscopy

Immunofluorescence microscopy was performed according to Brown et al. (2015) and Kubo et al. (2015). Cells adherent to poly-L lysine (Sigma)-coated coverslips were fixed in −20°C methanol for 15 min and air dried. Samples were doubly labeled with mouse monoclonal anti-acetylated-tubulin antibody (6-11B-1) and anti-IFT46 antibody (Hou et al., 2007) or rat monoclonal anti-HA antibody (3f10; Roche). Samples were treated with secondary antibodies conjugated with Alexa-Fluor-488 and Alexa-Fluor-594 (1:2000, Invitrogen).

The velocities and frequencies of IFT particles within flagella were determined by DIC microscopy as described previously (Kubo et al., 2015).

TIRF microscopy of fluorescently tagged α-tubulin

To generate strains expressing fluorescently tagged tubulin, *ift81-1 IFT81*, *ift81-1 IFT81(2E)*, *ift81-1 IFT81(5E)* and *ift74-2 IFT74Δ130* cells were transformed with the *Xba*I/*Kpn*I fragment of construct pBR25-sfGFP–α-tubulin (Craft et al., 2015). Colonies of transformants were picked from Tris-acetate-phosphate agar plates containing 10 µg/ml zeocin, and strains that had similar expression levels of sfGFP–α-tubulin were selected (see Fig. S3).

For TIRF microscopy of tubulin transport, we used a custom-built TIRF/epi-fluorescence structure-illumination microscope (TESM; Navaroli et al., 2012) with 100-mW diode lasers emitting at 491 nm and 561 nm, and equipped with a 525/50-nm emission filter. Cells were deflagellated by pH shock (Rosenbaum et al., 1969) and the cells with regenerating flagella were then attached to 0.01% poly-L-lysine-treated coverslips (Warner Instruments, MA; #1.5 thickness, 25-mm diameter). The experiments were carried out at room temperature. Flagella attached to the coverslip were partially photobleached by using a 491-nm epifluorescence beam of ∼3.3 nm diameter. Images were recorded at 20 images/s for 25 s (photobleach occurred 5 s after the onset of the recording) and analyzed by ImageJ as described in Lechtreck (2013). To increase the contrast by ImageJ, 'Brightness/Contrast' of all movies was adjusted identically; the value of 'Maximum' was decreased from 255 to 185. Supplementary movies (Movies 1–4) are played at 60 images/s (3× real time).

Measurement of flagellar length and assessment of swimming velocity

To determine flagellar regeneration kinetics, cells were deflagellated by pH shock (Rosenbaum et al., 1969). Subsequently, aliquots of cells were removed and fixed with 1% glutaraldehyde at 15-min intervals up to 135 min after deflagellation, and observed by using an inverted microscope. One flagellum each on at least 30 cells was measured in each experiment and the average flagella length was calculated.

Swimming velocity was measured by tracking images of moving cells recorded by means of bright-field microscopy using a 40× objective, 5× eyepiece and a digital camera incorporating a charge-coupled device. Recorded movies were processed using ImageJ to obtain average swimming velocities.

Acknowledgements

We thank Dr Haru-aki Yanagisawa (University of Tokyo, Japan) for providing the pLC8-MCS-aphVIII vector. We are grateful to Drs Gregory Hendricks and Lara Strittmatter (Core EM Facility, University of Massachusetts Medical School, Worcester, MA) for assistance with EM.

Competing interests

The authors declare no competing or financial interests.

Author contributions

T.K. and G.W. conceived and designed the experiments. K.L. and J.C. supplied constructs expressing tagged proteins. K.B. and K.F. set up the TIRF microscope. T.K., J.B. and K.B. collected the data. T.K., B.C., K.L. and G.W. analyzed and interpreted the data. T.K and G.W. wrote the paper.

Funding

This study was supported by a Uehara Memorial Foundation Research Fellowship for Research Abroad [to T.K.], a National Institutes of Health grant [grant number R37 GM030626 to G.B.W.], the Robert W. Booth Endowment at the University of Massachusetts Medical School [to G.B.W.], and a National Institutes of Health grant [grant number GM110413 to K.F.L.]. Deposited in PMC for release after 12 months.

Supplementary information

Supplementary information available online at
http://jcs.biologists.org/lookup/suppl/doi:10.1242/jcs.187120/-/DC1

References

Ahmed, N. T., Gao, C., Lucker, B. F., Cole, D. G. and Mitchell, D. R. (2008). ODA16 aids axonemal outer row dynein assembly through an interaction with the intraflagellar transport machinery. *J. Cell Biol.* **183**, 313-322.

Aldahmesh, M. A., Li, Y., Alhashem, A., Anazi, S., Alkuraya, H., Hashem, M., Awaji, A. A., Sogaty, S., Alkharashi, A., Alzahrani, S. et al. (2014). *IFT27*, encoding a small GTPase component of IFT particles, is mutated in a consanguineous family with Bardet-Biedl syndrome. *Hum. Mol. Genet.* **23**, 3307-3315.

Beales, P. L., Bland, E., Tobin, J. L., Bacchelli, C., Tuysuz, B., Hill, J., Rix, S., Pearson, C. G., Kai, M., Hartley, J. et al. (2007). *IFT80*, which encodes a conserved intraflagellar transport protein, is mutated in Jeune asphyxiating thoracic dystrophy. *Nat. Genet.* **39**, 727-729.

Berthold, P., Schmitt, R. and Mages, W. (2002). An engineered *Streptomyces hygroscopicus aph 7″* gene mediates dominant resistance against hygromycin B in *Chlamydomonas reinhardtii*. *Protist* **153**, 401-412.

Bhogaraju, S., Engel, B. D. and Lorentzen, E. (2013a). Intraflagellar transport complex structure and cargo interactions. *Cilia* **2**, 10.

Bhogaraju, S., Cajanek, L., Fort, C., Blisnick, T., Weber, K., Taschner, M., Mizuno, N., Lamla, S., Bastin, P., Nigg, E. A. et al. (2013b). Molecular basis of tubulin transport within the cilium by IFT74 and IFT81. *Science* **341**, 1009-1012.

Bhogaraju, S., Weber, K., Engel, B. D., Lechtreck, K.-F. and Lorentzen, E. (2014). Getting tubulin to the tip of the cilium: one IFT train, many different tubulin cargo-binding sites? *Bioessays* **36**, 463-467.

Brazelton, W. J., Amundsen, C. D., Silflow, C. D. and Lefebvre, P. A. (2001). The *bld1* mutation identifies the *Chlamydomonas osm-6* homolog as a gene required for flagellar assembly. *Curr. Biol.* **11**, 1591-1594.

Brown, J. M., DiPetrillo, C. G., Smith, E. F. and Witman, G. B. (2012). A FAP46 mutant provides new insights into the function and assembly of the C1d complex of the ciliary central apparatus. *J. Cell Sci.* **125**, 3904-3913.

Brown, J. M., Cochran, D. A., Craige, B., Kubo, T. and Witman, G. B. (2015). Assembly of IFT trains at the ciliary base depends on IFT74. *Curr. Biol.* **25**, 1583-1593.

Caparrós-Martín, J. A., De Luca, A., Cartault, F., Aglan, M., Temtamy, S., Otaify, G. A., Mehrez, M., Valencia, M., Vázquez, L., Alessandri, J.-L. et al. (2015). Specific variants in *WDR35* cause a distinctive form of Ellis-van Creveld syndrome by disrupting the recruitment of the EvC complex and SMO into the cilium. *Hum. Mol. Genet.* **24**, 4126-4137.

Castresana, J. and Saraste, M. (1995). Does Vav bind to F-actin through a CH domain? *FEBS Lett.* **374**, 149-151.

Ciferri, C., Pasqualato, S., Screpanti, E., Varetti, G., Santaguida, S., Dos Reis, G., Maiolica, A., Polka, J., De Luca, J. G., De Wulf, P. et al. (2008). Implications for kinetochore-microtubule attachment from the structure of an engineered Ndc80 complex. *Cell* **133**, 427-439.

Cole, D. G., Diener, D. R., Himelblau, A. L., Beech, P. L., Fuster, J. C. and Rosenbaum, J. L. (1998). *Chlamydomonas* kinesin-II-dependent intraflagellar transport (IFT): IFT particles contain proteins required for ciliary assembly in *Caenorhabditis elegans* sensory neurons. *J. Cell Biol.* **141**, 993-1008.

Craft, J. M., Harris, J. A., Hyman, S., Kner, P. and Lechtreck, K. F. (2015). Tubulin transport by IFT is upregulated during ciliary growth by a cilium-autonomous mechanism. *J. Cell Biol.* **208**, 223-237.

Craige, B., Tsao, C.-C., Diener, D. R., Hou, Y., Lechtreck, K.-F., Rosenbaum, J. L. and Witman, G. B. (2010). CEP290 tethers flagellar transition zone microtubules to the membrane and regulates flagellar protein content. *J. Cell Biol.* **190**, 927-940.

Dagoneau, N., Goulet, M., Geneviève, D., Sznajer, Y., Martinovic, J., Smithson, S., Huber, C., Baujat, G., Flori, E., Tecco, L. et al. (2009). *DYNC2H1* mutations cause asphyxiating thoracic dystrophy and short rib-polydactyly syndrome, type III. *Am. J. Hum. Genet.* **84**, 706-711.

Davis, E. E., Zhang, Q., Liu, Q., Diplas, B. H., Davey, L. M., Hartley, J., Stoetzel, C., Szymanska, K., Ramaswami, G., Logan, C. V. et al. (2011). *TTC21B*

contributes both causal and modifying alleles across the ciliopathy spectrum. *Nat. Genet.* **43**, 189-196.

Eguether, T., San Agustin, J. T., Keady, B. T., Jonassen, J. A., Liang, Y., Francis, R., Tobita, K., Johnson, C. A., Abdelhamed, Z. A., Lo, C. W. et al. (2014). IFT27 links the BBSome to IFT for maintenance of the ciliary signaling compartment. *Dev. Cell* **31**, 279-290.

Fowkes, M. E. and Mitchell, D. R. (1998). The role of preassembled cytoplasmic complexes in assembly of flagellar dynein subunits. *Mol. Biol. Cell* **9**, 2337-2347.

González-Ballester, D., de Montaigu, A., Galván, A. and Fernández, E. (2005). Restriction enzyme site-directed amplification PCR: a tool to identify regions flanking a marker DNA. *Anal. Biochem.* **340**, 330-335.

Gorman, D. S. and Levine, R. P. (1965). Cytochrome f and plastocyanin: their sequence in the photosynthetic electron transport chain of *Chlamydomonas reinhardti*. *Proc. Natl. Acad. Sci. USA* **54**, 1665-1669.

Halbritter, J., Bizet, A. A., Schmidts, M., Porath, J. D., Braun, D. A., Gee, H. Y., Mclnerney-Leo, A. M., Krug, P., Filhol, E., Davis, E. E. et al. (2013). Defects in the IFT-B component IFT172 cause Jeune and Mainzer-Saldino syndromes in humans. *Am. J. Hum. Genet.* **93**, 915-925.

Hao, L., Thein, M., Brust-Mascher, I., Civelekoglu-Scholey, G., Lu, Y., Acar, S., Prevo, B., Shaham, S. and Scholey, J. M. (2011). Intraflagellar transport delivers tubulin isotypes to sensory cilium middle and distal segments. *Nat. Cell Biol.* **13**, 790-798.

Harris, E. (2009). *The Chlamydomonas Sourcebook*, Vol. 1, 2nd edn. Amsterdam: Academic Press.

Hiller, G. and Weber, K. (1978). Radioimmunoassay for tubulin: a quantitative comparison of the tubulin content of different established tissue culture cells and tissues. *Cell* **14**, 795-804.

Hou, Y., Qin, H., Follit, J. A., Pazour, G. J., Rosenbaum, J. L. and Witman, G. B. (2007). Functional analysis of an individual IFT protein: IFT46 is required for transport of outer dynein arms into flagella. *J. Cell Biol.* **176**, 653-665.

Huber, C., Wu, S., Kim, A. S., Sigaudy, S., Sarukhanov, A., Serre, V., Baujat, G., Le Quan Sang, K.-H., Rimoin, D. L., Cohn, D. H. et al. (2013). *WDR34* mutations that cause short-rib polydactyly syndrome type III/severe asphyxiating thoracic dysplasia reveal a role for the NF-κB pathway in cilia. **93**, 926-931.

Ishikawa, H. and Marshall, W. F. (2011). Ciliogenesis: building the cell's antenna. *Nat. Rev. Mol. Cell. Biol.* **12**, 222-234.

Kamiya, R. (1988). Mutations at twelve independent loci result in absence of outer dynein arms in *Chlamydomonas reinhardtii*. *J. Cell Biol.* **107**, 2253-2258.

Kato-Minoura, T., Hirono, M. and Kamiya, R. (1997). *Chlamydomonas* inner-arm dynein mutant, *ida5*, has a mutation in an actin-encoding gene. *J. Cell Biol.* **137**, 649-656.

Kubo, T., Hirono, M., Aikawa, T., Kamiya, R. and Witman, G. B. (2015). Reduced tubulin polyglutamylation suppresses flagellar shortness in *Chlamydomonas*. *Mol. Biol. Cell* **26**, 2810-2822.

Lechtreck, K. F. (2013). In vivo imaging of IFT in *Chlamydomonas* flagella. *Methods Enzymol.* **524**, 265-284.

Lechtreck, K. F. (2015). IFT-cargo interactions and protein transport in cilia. *Trends Biochem. Sci.* **40**, 765-778.

Lechtreck, K.-F., Johnson, E. C., Sakai, T., Cochran, D., Ballif, B. A., Rush, J., Pazour, G. J., Ikebe, M. and Witman, G. B. (2009). The *Chlamydomonas reinhardtii* BBSome is an IFT cargo required for export of specific signaling proteins from flagella. *J. Cell Biol.* **187**, 1117-1132.

Lechtreck, K. F., Brown, J. M., Sampaio, J. L., Craft, J. M., Shevchenko, A., Evans, J. E., and Witman, G. B. (2013). Cycling of the signaling protein phospholipase D through cilia requires the BBSome only for the export phase. *J. Cell Biol.* **201**, 249-261.

Liem, K. F., Jr, Ashe, A., He, M., Satir, P., Moran, J., Beier, D., Wicking, C. and Anderson, K. V. (2012). The IFT-A complex regulates Shh signaling through cilia structure and membrane protein trafficking. *J. Cell Biol.* **197**, 789-800.

Liew, G. M., Ye, F., Nager, A. R., Murphy, J. P., Lee, J. S., Aguiar, M., Breslow, D. K., Gygi, S. P. and Nachury, M. V. (2014). The intraflagellar transport protein IFT27 promotes BBSome exit from cilia through the GTPase ARL6/BBS3. *Dev. Cell* **31**, 265-278.

Ling, L. and Goeddel, D. V. (2000). MIP-T3, a novel protein linking tumor necrosis factor receptor-associated factor 3 to the microtubule network. *J. Biol. Chem.* **275**, 23852-23860.

Lucker, B. F., Behal, R. H., Qin, H., Siron, L. C., Taggart, W. D., Rosembaum, J. L. and Cole, D. G. (2005). Characterization of the intraflagellar transport complex B core: direct interaction of the IFT81 and IFT74/72 subunits. *J. Biol. Chem.* **280**, 27688-27696.

Marshall, W. F. and Rosenbaum, J. L. (2001). Intraflagellar transport balances continuous turnover of outer doublet microtubules: implications for flagellar length control. *J. Cell Biol.* **155**, 405-414.

Mclnerney-Leo, A. M., Schmidts, M., Cortés, C. R., Leo, P. J., Gener, B., Courtney, A. D., Gardiner, B., Harris, J. A., Lu, Y., Marshall, M. et al. (2013). Short-rib polydactyly and Jeune syndromes are caused by mutations in *WDR60*. *Am. J. Hum. Genet.* **93**, 515-523.

Merrill, A. E., Merriman, B., Farrington-Rock, C., Camacho, N., Sebald, E. T., Funari, V. A., Schibler, M. J., Firestein, M. H., Cohn, Z. A., Priore, M. A. et al. (2009). Ciliary abnormalities due to defects in the retrograde transport protein DYNC2H1 in short-rib polydactyly syndrome. *Am. J. Hum. Genet.* **84**, 542-549.

Navaroli, D. M., Bellve, K. D., Standley, C., Lifshitz, L. M., Cardia, J., Lambright, D., Leonard, D., Forgarty, K. E. and Corvera, S. (2012). Rabenosyn-5 defines the fate of the transferrin receptor following clathrin-mediated endocytosis. *Proc. Natl. Acad. Sci. USA* **109**, E471-E480.

Perrault, I., Saunier, S., Hanein, S., Filhol, E., Bizet, A. A., Collins, F., Salih, M. A. M., Gerber, S., Delphin, N., Bigot, K. et al. (2012). Mainzer-Saldino syndrome is a ciliopathy caused by *IFT140* mutations. *Am. J. Hum. Genet.* **90**, 864-870.

Perrault, I., Halbritter, J., Porath, J. D., Gérard, X., Braun, D. A., Gee, H. Y., Fathy, H. M., Saunier, S., Cormier-Daire, V., Thomas, S. et al. (2015). *IFT81*, encoding an IFT-B core protein, as a very rare cause of a ciliopathy phenotype. *J. Med. Genet.* **52**, 657-665.

Piperno, G., Mead, K. and Henderson, S. (1996). Inner dynein arms but not outer dynein arms require the activity of kinesin homologue protein KHP1(FLA10) to reach the distal part of flagella in *Chlamydomonas*. *J. Cell. Biol.* **133**, 371-379.

Richey, E. A. and Qin, H. (2012). Dissecting the sequential assembly and localization of intraflagellar transport particle complex B in *Chlamydomonas*. *PLoS ONE* **7**, e43118.

Rosenbaum, J. L. and Witman, G. B. (2002). Intraflagellar transport. *Nat. Rev. Mol. Cell. Biol.* **3**, 813-825.

Rosenbaum, J. L., Moulder, J. E. and Ringo, D. L. (1969). Flagellar elongation and shortening in *Chlamydomonas*: the use of cycloheximide and colchicine to study the synthesis and assembly of flagellar proteins. *J. Cell Biol.* **41**, 600-619.

Sager, R. and Granick, S. (1954). Nutritional control of sexuality in *Chlamydomonas reinhardi*. *J. Gen. Physiol.* **37**, 729-742.

Schmidts, M., Arts, H. H., Bongers, E. M. H. F., Yap, Z., Oud, M. M., Antony, D., Duijkers, L., Emes, R. D., Stalker, J., Yntema, J.-B. et al. (2013). Exome sequencing identifies *DYNC2H1* mutations as a common cause of asphyxiating thoracic dystrophy (Jeune syndrome) without major polydactyly, renal or retinal involvement. *J. Med. Genet.* **50**, 309-323.

Schmidts, M., Hou, Y., Cortés, C. R., Mans, D. A., Huber, C., Boldt, K., Patel, M., van Reeuwijk, J., Plaza, J.-M., van Beersum, S. E. C. et al. (2015). *TCTEX1D2* mutations underlie Jeune asphyxiating thoracic dystrophy with impaired retrograde intraflagellar transport. *Nat. Commun.* **6**, 7074.

Scholey, J. M. (2008). Intraflagellar transport motors in cilia: moving along the cell's antenna. *J. Cell Biol.* **180**, 23-29.

Silflow, C. D., LaVoie, M., Tam, L.-W., Tousey, S., Sanders, M., Wu, W.-C., Borodovsky, M. and Lefebvre, P. A. (2001). The Vfl1 protein in *Chlamydomonas* localizes in a rotationally asymmetric pattern at the distal ends of the basal bodies. *J. Cell Biol.* **153**, 63-74

Taschner, M., Bhogaraju, S., Vetter, M., Morawetz, M. and Lorentzen, E. (2011). Biochemical mapping of interactions within the intraflagellar transport (IFT) B core complex: IFT52 binds directly to four other IFT-B subunits. *J. Biol. Chem.* **286**, 26344-26352.

Taschner, M., Weber, K., Mourão, A., Vetter, M., Awasthi, M., Stiegler, M., Bhogaraju, S. and Lorentzen, E. (2016). Intraflagellar transport proteins 172, 80, 57, 54, 38, and 20 form a stable tubulin-binding IFT-B2 complex. *EMBO. J.* **35**, 773-790.

Towbin, H., Staehelin, T. and Gordon, J. (1979). Electrophoretic transfer of proteins from polyacrylamide gels to nitrocellulose sheets: procedure and some applications. *Proc. Natl. Acad. Sci. USA* **76**, 4350-4354.

Wang, Q., Pan, J. and Snell, W. J. (2006). Intraflagellar transport particles participate directly in cilium-generated signaling in Chlamydomonas. *Cell* **125**, 549-562.

Witman, G. B., Plummer, J. and Sander, G. (1978). *Chlamydomonas* flagellar mutants lacking radial spokes and central tubules. Structure, composition, and function of specific axonemal components. *J. Cell Biol.* **76**, 729-747.